Iranian Polymer Journal (2021) 30:1019–1028
https://doi.org/10.1007/s13726-021-00952-7

ORIGINAL RESEARCH

Synthesis, rheological characterization, and antibacterial activity of polyvinyl alcohol (PVA)/ zinc oxide nanoparticles wound dressing, achieved under electron beam irradiation

Mina Arab[1] · Mojtaba Jallab[1] · Mehdi Ghaffari[1] · Ehsan Moghbelli[2] · Mohammad Reza Saeb[3]

Received: 21 November 2020 / Accepted: 9 May 2021 / Published online: 22 June 2021

Abstract
An antibacterial wound dressing hydrogel was synthesized from biopolymers and a semiconductor nanomaterial by gamma irradiation, and applied in a simulated environment. Polyvinyl alcohol (PVA)/agar hydrogel was chosen due to its biocompatibility and good swelling to absorb wound exudates and make a moist environment to accelerate the wound healing process. Zinc oxide nanoparticles were synthesized and combined with the hydrogel due to their antibacterial activity as a wound dressing aid and the hydrophilic nature to enhance swelling capacity by facilitating water flow in the hydrogel. Hydrogel samples based on PVA/agar containing low amounts of zinc oxide nanoparticles were prepared by gamma irradiation to meet all the requirements of a wound dressing. Water absorption, swelling behavior and pH sensitivity were studied and showed an excellent water swelling capacity. Scanning electron microscopy (SEM) and UV–Vis spectroscopy analyses were employed, where dispersion state of nanoparticles played a key role. Antibacterial activity mechanisms and the resistance to gram-positive bacteria were tested by the disk diffusion method, and the developed hydrogel revealed resistance against gram-positive bacteria. A cone and plate rheometer was used to capture the rheological response of hydrogel. Reduction in viscosity and elastic modulus was due to increasing the amount of zinc oxide nanoparticles. Analyses on mechanical properties approved that hydrogels had enough strength for wound dressing to resist tear once stretched.

✉ Mehdi Ghaffari
m.ghaffari@gu.ac.ir

[1] Department of Polymer Engineering, Faculty of Engineering, Golestan University, Gorgan, Iran

[2] Polymer Technology Center, Department of Materials Science and Engineering, Texas A&M University, College Station, TX 77843, USA

[3] Department of Resin and Additives, Institute for Color Science and Technology, P.O. Box 16765-654, Tehran, Iran

Graphic abstract

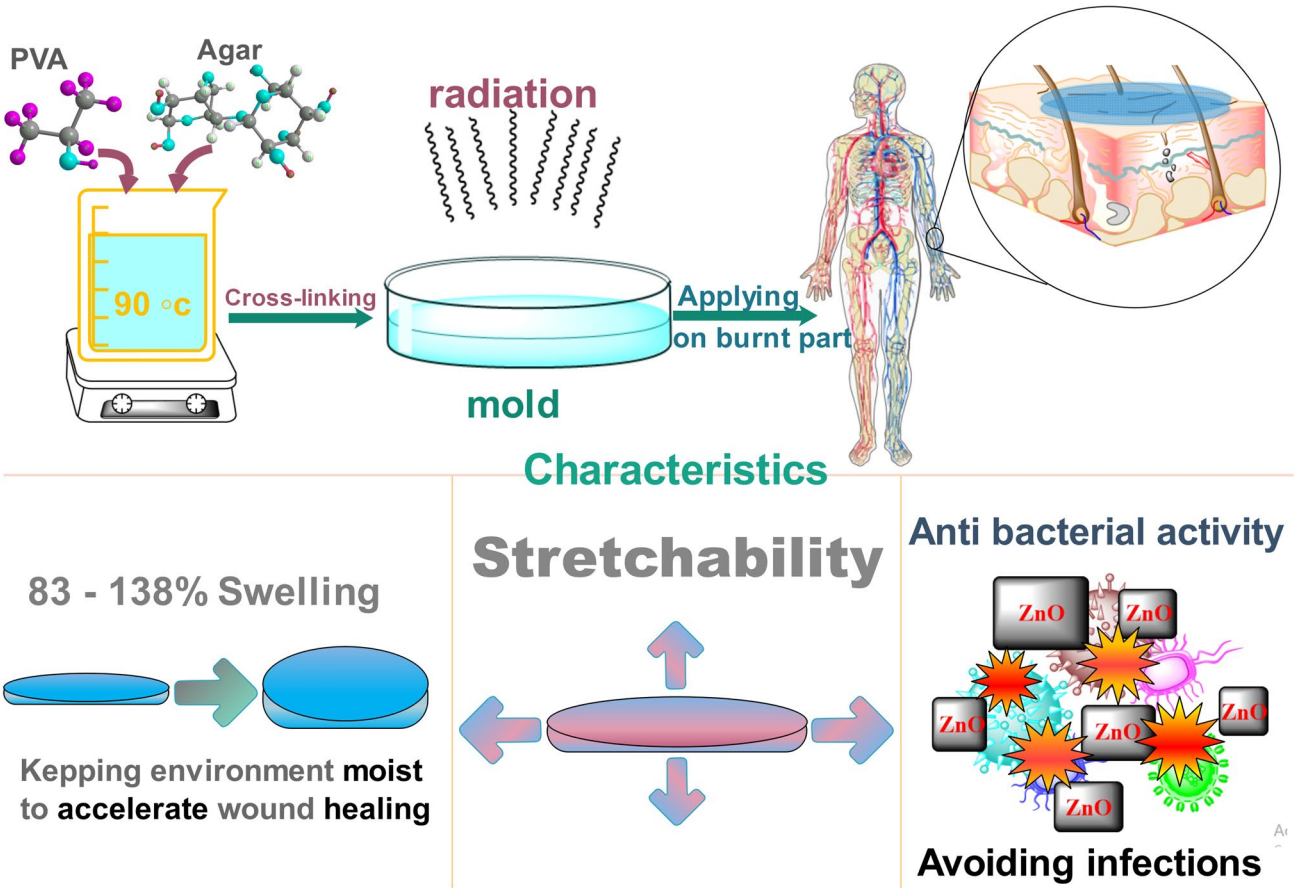

Keywords Wound dressing · Burn wound treatment · Biohydrogel · Electron beam irradiation · Zinc oxide nanoparticle

Introduction

For years, dressing has been used for wound healing and some materials such as medical absorbent cotton and pledget have been conventionally used to isolate a wound from the surrounding environment. With developments in technology, wound healing experienced an evolutionary period in a series of stages. Winter et al. [1] demonstrated that wound healing can be faster in a moist environment than that under dry conditions. Such an important outcome encouraged researchers to define strategies for fast healing. So that, in recent research the focus is placed on developing new kinds of moist dressings [2]. Hence, moist dressings were expected to provide the growth factors with conditions to avoid tissue dehydration and cell death [3]. It was also recognized that shedding could induce loss of the stratum corneum resulting in a large amount of trans-epidermal water loss, where conventional dressings could complicate this process [4, 5]. During wound healing, barrier formation appears as a critical process and moist wound healing can avoid this process by assuring keratinocytes proliferation, migration, and differentiation [6]. Furthermore, the re-epithelization rate of tissue can increase remarkably and these factors can accelerate wound healing [7].

Materials selection for moist dressing depends on the type of wound and the corresponding treatment period [8]. Several studies have attempted to find a suitable candidate to fulfill the requirements for wound healing where hydrogels appeared promising among other candidates due to their auspicious characteristics such as prompt pain control, absorbing modest amounts of body fluids, excellent antibacterial activity, simple replacement, good breathability and good handling [9, 10]. Hydrogels are networks of macromolecules and sometimes colloidal gels with hydrophilic nature that are used as biomaterials in wound dressing, drug delivery systems, transdermal systems, dental applications, injectable polymers, implants, soft contact lenses, superabsorbent, and stimuli-responsive systems [11, 12]. Several hydrogels based

on various natural polymers or their derivatives, e.g., starch [13], gelatin [14], chitosan [15], carboxymethyl cellulose [16], sodium alginate [17], along with synthetic polymers, e.g., polyvinyl alcohol (PVA) and polyvinyl pyrrolidone (PVP) have been widely used as a wound dressing and biomedical applications [18, 19]. Nevertheless, poor mechanical properties of natural polymers from one side and limited biodegradability of synthetic polymers from the other side directed attention towards the use of hybrid systems [20].

PVA is a water-soluble polyhydroxyl that in the form of hydrogel is knows as a biomaterial [21, 22]. Due to its non-toxicity, biocompatibility, biodegradability, non-carcinogenic property, facile synthesis route, excellent chemical resistance, proper physical properties, gelation ability, and low price [11, 23], PVA has been widely considered in biomedical and pharmaceutical applications [24, 25]. One of the most important properties of hydrogels is the ability to absorb wound exudates, where the pH of media can change the swelling rate [26, 27]. For healthy adults and children, the pH of skin was reported to take a value in the close proximity of five, while by progress in healing the pH will change accompanied by a change in the swelling rate [28]. In addition, an increase in pH facilitates the propagation of bacteria and changes the type of bacteria [29]. Studies on burn wound healing, especially in second-degree burning, demonstrated some important factors that can change the pH such as infections and burn depth [30]. Thus, advanced wound dressing protocols attempted to trigger such fluctuations in the period of treatment.

Different methods have been reported for the preparation of hydrogels, consisting of chemical methods by a covalent cross-linking agent [31], physical methods by a complexing agent, and radiation methods by gamma-radiation [32], electron beams, and ultraviolet light [33, 34]. In recent years, many studies have reported on wound dressing hydrogels that were prepared by irradiation method [35, 36]**.** Among the aforementioned methods, irradiation techniques were identified as the most convenient for improving and modifying wound dressings by grafting, degradation, or crosslinking. Chemical crosslinking is a highly versatile method to modify the mechanical, thermal, and chemical stability of polymer hydrogels [37]. In this method, a stabilized network structure is formed in which chains are linked chemically [38]. Crosslinking by irradiation uses high energy radiation like X-ray, gamma, or electron beam to make covalent bonding between chains [34, 39].

Hydrogels can be treated into physical and chemical structures based on their crosslinking mechanism [38]. Physical crosslinks are formed through entangled chains, hydrogen bonds, hydrophobic interactions, and crystalline formation, but temporarily keep hydrogels insoluble [40, 41]. Polymerization by gamma irradiation uses high energy as the main factor to crosslink water-soluble monomers or chains without any crosslinking agent with toxic nature or undesired reactions taking place in the bulk of hydrogel [32]. In this method, free radical polymerization creates hydroxyl radicals of alcohol and vinyl monomers as initiators leading to a 3D network formation once the gelation point is reached [40, 42].

Herein, based on the preference for the radiation method to perfectly cross-link the hydrogel, PVA/agar biohydrogel was synthesized by gamma irradiation. Synthesized zinc oxide nanoparticles were dispersed in the matrix to increase swelling capacity due to hydrophilic nature and facilitating water flow inside the hydrogel pours and also giving antibacterial properties. The rheological analysis is one of the less subjected characteristics for wound dressings that have an important role in characterizing and managing the properties. Therefore, rheological measurements were carried out to investigate viscosity, elastic moduli, and frequency dependence of hydrogels. To be applicable as wound dressing, hydrogels passed the mechanical tests exhibiting the required extent of stretching. Water absorption, swelling behavior, and sensitivity to pH stimuli of hydrogels render them appropriate for use as wound dressing under various conditions.

Experimental

Materials

In this study, polyvinyl alcohol (PVA) with an average molecular weight of 72,000 and ZnO nanoparticles (ZnONPs) with an average size of 40 nm were purchased from Merck and Sigma Aldrich, respectively. Agar was obtained from BD BactoCompany (America) to improve the mechanical properties of nanocomposites.

Preparation of PVA/ZnO nanocomposites

To prepare PVA/ZnO nanocomposite, 3.5 g of polyvinyl alcohol was dissolved in 90 mL of distilled water at 90 °C. PVA solution was stirred for 4 h at 90–95 °C until the prepared solution became clear and homogeneous. Thereafter,1 g agar was added to PVA solution and stirred for 1 h. Afterward, varying amounts of ZnO nanoparticles (0.05, 0.1, 0.2% by wt) were added to the solution. For degassing, the solution was situated in an ultrasonic bath for 20 min at 80 °C and then poured into the mold.

Cross-linking of PVA/agar nanocomposites

The prepared gel sample was placed in aluminum foil and subjected to a 10 MeV accelerator. The absorbed dose was probed by the appropriate speed of the conveyor. To ensure

an adsorbed dosage of samples, calibrated triacetate cellulose film was used. In this study, samples were irradiated at 25 kGy.

Methods

Rheological studies

Rheological shear measurements were performed using an Anton Paar physical shear rheometer (MCR300) using a parallel plate geometry with a 25 mm plate diameter. The frequency sweep range of 0.1–100 rad/s was conducted with a strain amplitude of 0.2% at room temperature and under air atmosphere.

Scanning electron microscopy

The morphology of PVA/ZnO nanocomposite was investigated by scanning electron microscopy (SEM, TESCAN, Czech). To prevent morphological changes, the samples were placed in liquid nitrogen for one minute then fractured, whereupon a layer of gold was coated on the fracture surface to be analyzed by SEM.

UV–VIS spectroscopy

The UV–Vis spectra absorption of PVA/ZnO nanocomposites were measured (PG instrument T90, England). The pure sample and samples containing different amounts of ZnO nanoparticles were investigated at visible wavelengths of 100–600 nm.

Band gap energy (Eg) was estimated by Tauc's relationship (Eq. 1):

$$(\alpha hv) = B(hv - \mathrm{Eg})^n, \tag{1}$$

where, α is the optical absorption coefficient, B is a constant factor that depends on transition probability, hv is related to light energy and n is the electronic transition number.

Antimicrobial studies

Antibacterial activity of PVA/ZnO nanocomposite was studied using disk diffusion method on gram-positive bacteria strain, *Bacillus subtilis* (*B. subtilis*). The freshly cultured bacteria in a phosphate buffer was used to prepare a suspension containing $1–1.5 \times 10^8$ Cru/mL (McFarland). The suspension was cultured on Muller Hinton agar culture medium by surface cultivation method. The prepared hydrogels containing 0.05, 0.1, and 0.2% (wt) ZnO NPs and the sample without ZnO, at the sterile condition, were cut into 0.5 cm discs. Afterward, they were placed on the incubated culture medium surface and heated for 24 h at 37 °C in a bacteriological incubator. Finally, after the incubation process, the environment was analyzed for the presence of an inhibition zone where the inhibition zone diameter was also assessed.

Mechanical test

The mechanical behavior of hydrogels was evaluated by a uniaxial tensile test machine (Gotech, Taiwan). The elongation-at-break/tear point was determined. Sample thickness equivalent to 2 mm, testing at ambient temperature, at a 50 mm/min crosshead speed was utilized.

Swelling test

At first, hydrogels were dried and their weights were determined after immersion in distilled water for 48 h at room temperature. To determine the swelling rate, before measurements, hydrogels surface water was dried using paper. The swelling rate was calculated by Eq. (2) shown below:

$$\text{Swelling rate}\,(\%) = \frac{w_\mathrm{S} - w_\mathrm{d}}{w_\mathrm{d}} \times 100, \tag{2}$$

where, w_d and w_S are dry and swollen cube weights, respectively.

Results and discussion

Swelling behavior

Recent studies have shown the pH effect on wound healing [30]. After progress in wound healing, the pH becomes neutral or even acidic [30]. It should be noted that chronic wounds have a pH range of 7.15–8.9 [30]. In second-degree burns, the wound pH range is 8–8.5 at the beginning, and by passing each stage of healing, a different pH will be reached ranging from 6.5 to 9. Factors such as infections and wound depthcan affect pH and swelling rate [43]. Hence, the porosity of hydrogel helps to absorb wound exudates to reduce infections [6] and to provide a wet environment [44]. Therefore, hydrogels swelling behavior was studied in pH values of 2, 4, 7 and 9. As shown in Fig. 5, maximum swelling varies in each pH value for different nanoparticle percentages. Nonetheless, the grade and stage of a wound are important factors to choose the best nanoparticles percentage. The relationship between swelling and time of immersion has been presented in Figs. 1, 2, 3, 4 where the progress of swelling ratio with time can be seen. It can be understood that all samples have the same swelling pattern. Swelling rate is high at the beginning and then slows down [45]. In Fig. 5, maximum swelling based on pH value and

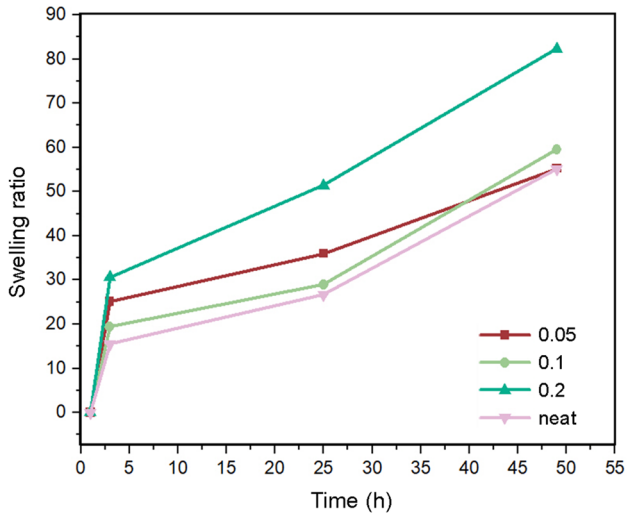

Fig. 1 Swelling ratio of PVA/agar hydrogel composed of 0.05, 0.1 and 0.2% (wt) ZnO NPs at pH 2

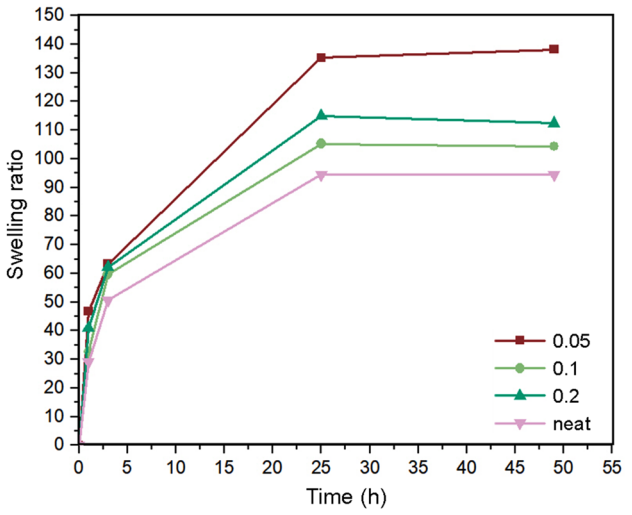

Fig. 3 Swelling ratio of PVA/agar hydrogel composed of 0.05, 0.1 and 0.2% (wt) ZnO NPs at pH 7

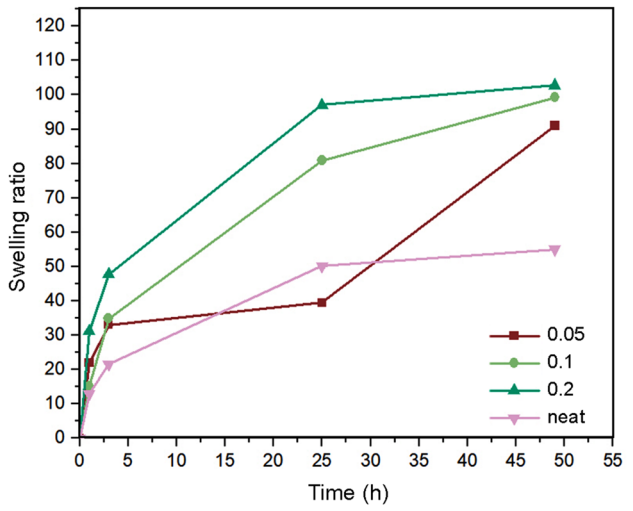

Fig. 2 Swelling ratio of PVA/agar hydrogel composed of 0.05, 0.1 and 0.2% (wt) ZnO NPs at pH 4

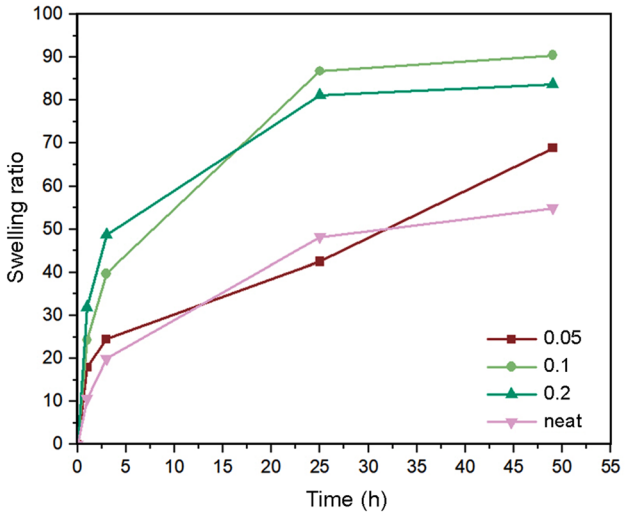

Fig. 4 Swelling ratio of PVA/agar hydrogel composed of 0.05, 0.1 and 0.2% (wt) ZnO NPs at pH 9

nanoparticle percentages has been presented. The highest swelling belongs to 0.05% (wt) ZnO NPs at pH 7 but in the case of chronic wounds and second-degree burn wounds, 0.1% (wt) shows better swelling due to the alkaline pH of the wound.

Rheological behavior

Storage modulus, loss modulus, complex viscosity, and damping (tan δ) curves versus frequency for the hydrogel samples with various amounts of ZnO nanoparticles are shown in Figs. 6, 7, 8, 9, respectively. According to these results, all the hydrogel samples have solid-like rheological behavior that could imply a network structure such as cross-links. The results revealed the incorporation of the nanoparticles at most frequencies. Although, the values of these properties are larger than those for neat hydrogel at high frequencies. The reduction in rheological properties of hydrogel nanocomposites could indicate a decrease in the chemical cross-link density of hydrogels in the presence of nanoparticles. This would be in agreement with the previously observed increase in swelling values of hydrogel, due to nanoparticle addition (Fig. 5).

In addition, observed increments in rheological properties of hydrogel nanocomposite at high frequencies maybe attributed to potential electrostatic interactions of nanoparticles

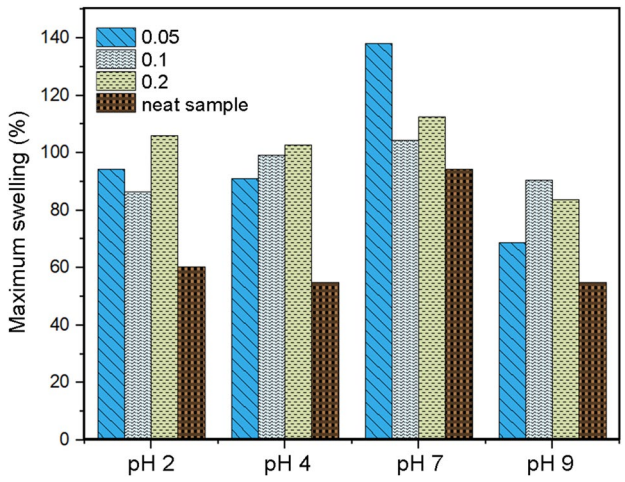

Fig. 5 Maximum swelling of the hydrogel with 0.05, 0.1 and 0.2% (wt) ZnO NPs in different pH values

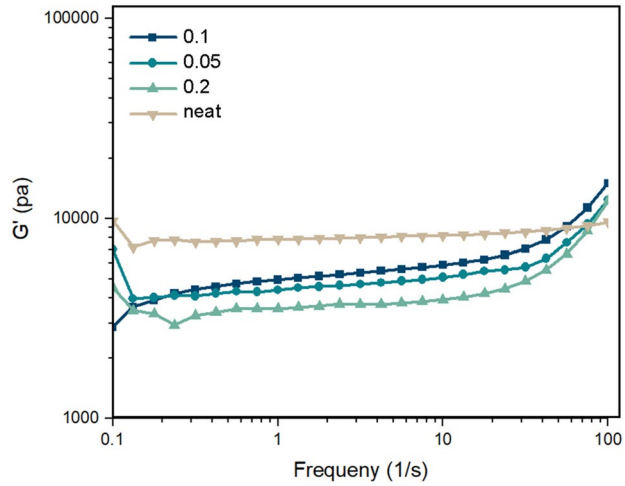

Fig. 6 Storage modulus of the hydrogel with 0.05, 0.1and 0.2% (wt) ZnO NPs

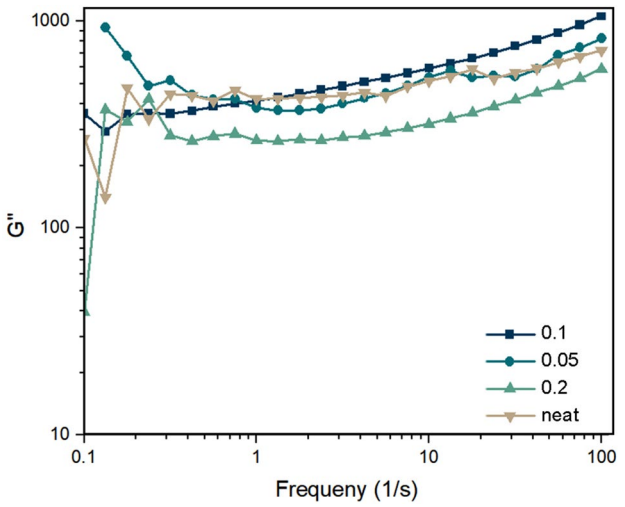

Fig. 7 Loss modulus of the hydrogel with 0.05, 0.1 and 0.2% (wt) ZnO NPs

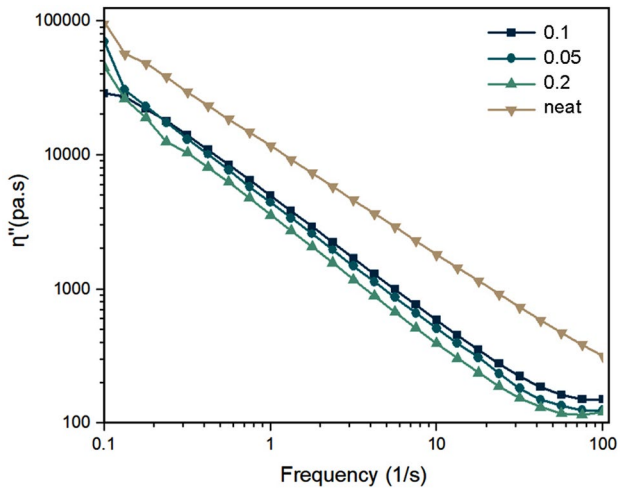

Fig. 8 Hydrogels viscosity with 0.05, 0.1 and 0.2% (wt) ZnO NPs

and polymer chains within the hydrogel matrix. At high frequencies, i.e., the short relaxation time for polymer chains, electrostatic interactions act as physical cross-links between polymer chains. This compensates for the lack of chemical cross-links of PVA polymer, which may be the source of enhanced viscoelastic properties at high frequencies. At low frequencies when providing enough time, the short-range relaxation time of chains can relate to their electrostatic interactions with nanoparticles. These relaxations are confirmed by peaks that appeared in tan δ curves in the frequency ranges of 20–50 rad/s, while there is no obvious peak at the same frequency range for neat hydrogel (Fig. 9). The noteworthy subject in rheological properties of hydrogel nanocomposite samples is the dual role effect of nanoparticles upon viscoelastic properties. This is disclosed by considering that the lowest values of the viscoelastic properties are for 0.2% (wt) ZnO.

This trend of changes in the viscoelastic properties of samples could be explained by nanoparticles induced alternations in the type and density of cross-links. As mentioned before, the presence of nanoparticles reduces chemical cross-link density. Therefore, it reduces the viscoelastic properties. On the other hand, it increases the possibility of physical cross-links formation and viscoelastic properties increment.

Nevertheless, how each of these opposite impacts of nanoparticle influencing the viscoelastic properties depends on their amounts and state of dispersion within the hydrogel [10].

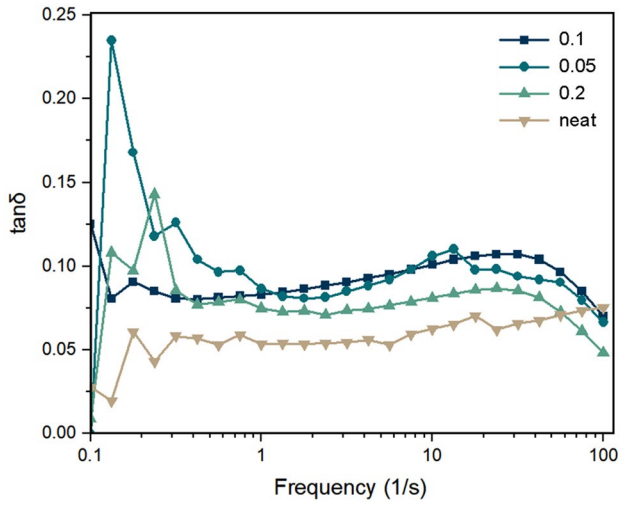

Fig. 9 Damping term of the hydrogel with 0.05, 0.1 and 0.2% (wt) ZnO NPs

Scanning electron microscopy (SEM)

Scanning electron microscopy was used to determine the dispersion, distribution, and particle size of ZnO NPs in the PVA matrix. According to mapping analysis (Fig. 10), ZnO NPs showed good dispersion and well distributed throughout the matrix. It also can be seen that particles are in nano size. By increasing ZnO content to 0.2% (wt), a slight aggregation was observed in some parts.

UV–Vis spectroscopy

To further prove the presence, dispersion, and nanosize of nanoparticles in the whole network, UV–Vis spectral results were investigated [44]. All of the spectrums that contained ZnO NPs were between 300 and 400 nm, which is due to surface plasmon resonance (SPR). As shown in Fig. 11, the absorption peak at 334 nm confirmed the presence of ZnO NPs. The higher percentage of ZnO NPs increased peak intensity as well as the intensity of plasma bands shifted to higher wavelength numbers. According to Fig. 11, it is obvious that the highest absorption peak belongs to 0.2% (wt) ZnO NPs.

To the best of our knowledge, better dispersion of NPs increases interactions and hydrogen bonds between the phases [46, 47]. This phenomenon results in increasing the band gap energy (Fig. 12).

As estimated from the plot, band gap energies for 0.05, 0.1 and 0.2% (wt) ZnO NPs were 3.47, 3.46 and 3.45 eV, respectively. Values of 3.4 eV [48, 49] and 3.5 eV [46] have been reported for band gap energy of nanosize ZnO, which matches with estimated values in this work. This proves that ZnO NPs are in nanosize and well dispersed in the whole matrix.

Antibacterial studies

For bacteria, the cell wall is located outside the cell membrane and composed of a layer of peptidoglycan (Fig. 13a). The structure of gram-positive bacteria consists of one cytoplasmic membrane with peptidoglycan layers and a thick cell wall. While, gram-negative bacteria having wall with two cell membranes, an outer membrane and a plasma membrane with a thick peptidoglycan layer [23].

Possible antibacterial mechanisms of ZnO NPs can be classified as theliberation of Zn^{2+} ions [33], formation of ROS (reactive oxygen species: H_2O_2, OH^-, O_2^-) and creation of electrostatic forces between bacteria and ZnO (Fig. 13) [23, 33]. In the ROS formation mechanism, oxidizing property and high reactivity are reasons for antibacterial activity. Reactive oxygen species can pass through the cell wall, damaging bacterial cell wall and causing cytoplasmic content leakage to destroy and killing bacteria [23, 50].

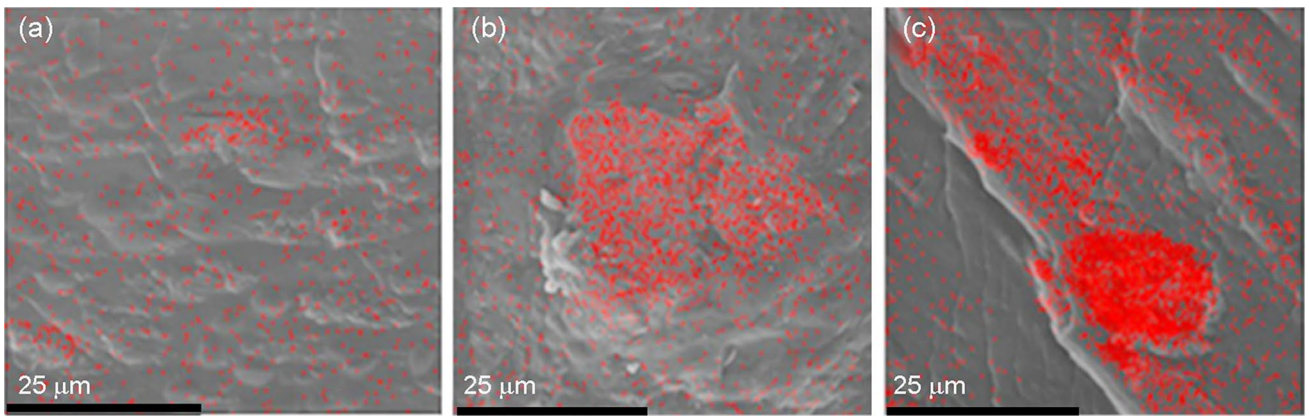

Fig. 10 SEM images of the hydrogel samples: **a** 0.05, **b** 0.1 and **c** 0.2% (wt) of ZnO NPs

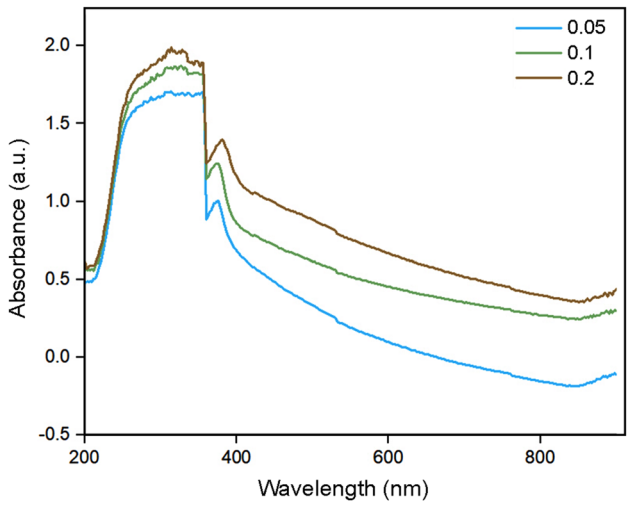

Fig. 11 UV–VIS absorption peaks of the hydrogels containing 0.05, 0.1 and 0.2% (wt) ZnO NPs

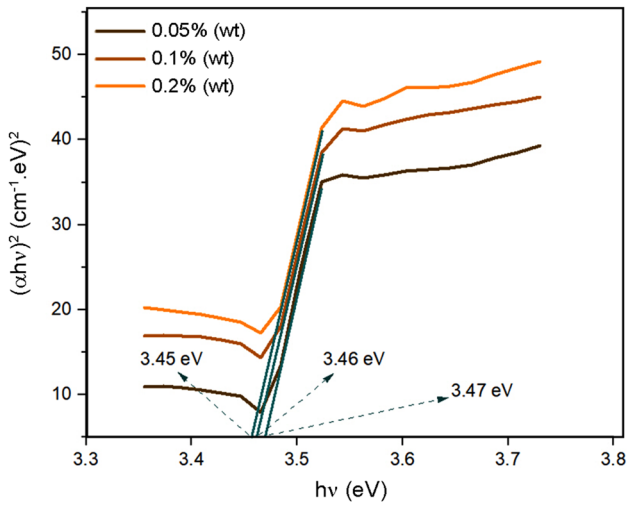

Fig. 12 Band gap energy of the samples with 0.05, 0.1 and 0.2% (wt) ZnO NPs

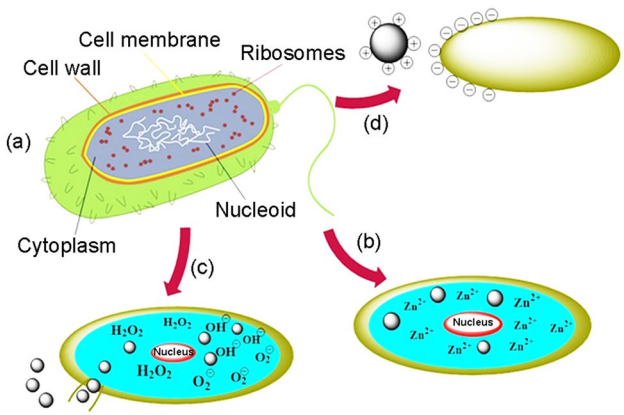

Fig. 13 Antibacterial mechanisms: **a** structure of bacteria, **b** liberation of Zn^{2+}, **c** ROS formation, and **d** electrostatic forces between ZnO NPs and bacteria

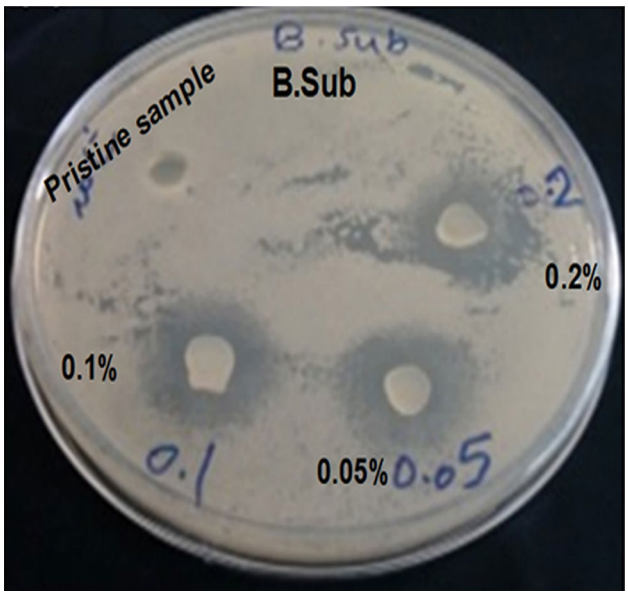

Fig. 14 Antibacterial test against *B. subtilis* bacteria

Hence, we carried out antibacterial tests to analyze the strength of hydrogel nanocomposite against gram-positive bacteria, which is infection and contamination index. In different studies, hydrogel-containing ZnO nanoparticles had resistance to gram-negative and gram-positive bacteria. However, the inhibition zone was different among bacteria and gram-positive bacteria showed less resistance to ZnO nanoparticles, which may lead to the destruction of the cell membrane due to the generation of hydrogen peroxide. Another reason for this phenomenon is the photocatalytic integration of zinc oxide. Usually, by increasing the amount of zinc oxide, the resistance of bacteria will be increased, which this increase in resistance is more for gram-negative than gram-positive bacteria. According to Fig. 14, resistance to *B. subtilis* bacteria for all samples with different amounts of ZnO nanoparticles was observed and the inhibition zone had no significant change for samples containing ZnO NPs.

Mechanical properties of PVA/ZnO nanocomposites

The wound dressing is in contact with the skin and does not tear easily when stretched [11]. Tensile strength was seen to increase when the amounts of nanoparticles increased, due to interactions of hydrogel and ZnONPs, which cause an increase in macromolecular movements between chains [51]. Therefore, it results in an increase in

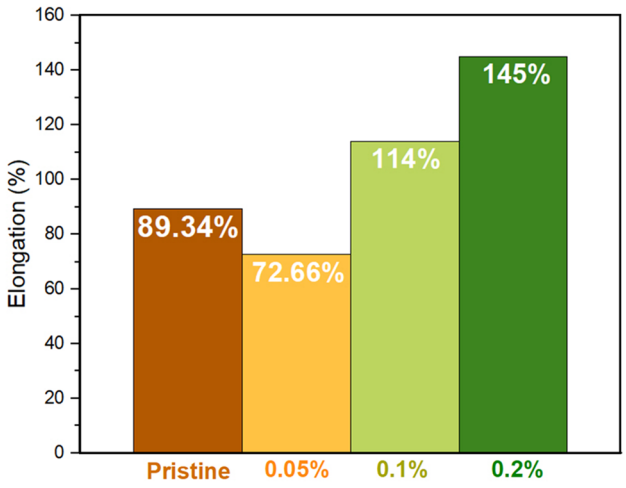

Fig. 15 Elongation-at-break for the pristine and samples containing 0.05, 0.1 and 0.2% (wt) ZnO NPs

elongation due to interactions between ZnO and PVA [10] and weakens the intermolecular hydrogen bonds of PVA and agar. It also makes new hydrogen bonds between PVA and ZnO and facilitates the macromolecular movements of chains. According to Fig. 15, the addition of 0.05% (wt) ZnO NPs decreased elongation but by increasing the content to 0.1 and 0.2% (wt) ZnO NPs, elongation had an increase. The elongation reached 140% as the maximum for 0.2% (wt) ZnO NPS. With respect to the values, the prepared hydrogel showed great tensile properties and could be stretched with body movements when applied to the skin.

Conclusion

PVA/ZnO hydrogel was synthesized for wound dressing. The prepared hydrogels were characterized by SEM micrographs, UV–Vis spectra, swelling tests, rheological behavior, and mechanical tests as well as antibacterial activity. The results from SEM images showed good distribution and dispersion of nanosize particles. UV–Vis test was used to prove good dispersion and presence of nanosize particles in the whole matrix. Swelling rate measurements showed values between 70 and 138% and demonstrated good swelling behavior in both acidic and alkaline environments, which can operate in all stages of the healing process. Antibacterial activity evaluation resulted in resistance of hydrogels to gram-positive *B. subtilis* bacteria. In conclusion, supported by the obtained properties and results the hydrogels have antibacterial activity, good swelling behavior, and significant mechanical properties that make them a great potential for wound healing applications.

References

1. Winter GD (1962) Formation of the scab and the rate of epithelization of superficial wounds in the skin of the young domestic pig. Nature 193:293
2. Kapanya A, Somsunan R, Phasayavan W, Molloy R, Jiranusornkul S (2020) Effect of molecular weight of poly (ethylene glycol) as humectant in interpenetrating polymer network hydrogels based on poly (sodium AMPS) and gelatin for wound dressing applications. Int J Polym Mater Polym Biomater 70:496–506
3. Field CK, Kerstein MD (1994) Overview of wound healing in a moist environment. Am J Surg 167:S2–S6
4. Wallace LA, Gwynne L, Jenkins T (2019) Challenges and opportunities of pH in chronic wounds. Ther Deliv 10:719–735
5. Debele TA, Su WP (2020) Polysaccharide and protein-based functional wound dressing materials and applications. Int J Polym Mater Polym Biomater 17:1–22
6. Kumar P, Lakshmanan VK, Biswas R, Nair SV, Jayakumar R (2012) Synthesis and biological evaluation of chitin hydrogel/nano ZnO composite bandage as antibacterial wound dressing. J Biomed Nanotechnol 8:891–900
7. Tsai HC, Shu HC, Huang LC, Chen CM (2019) A randomized clinical trial comparing a collagen-based composite dressing versus topical antibiotic ointment on healing full-thickness skin wounds to promote epithelialization. Formosan J Surg 52:52
8. Balakrishnan B, Mohanty M, Umashankar P, Jayakrishnan A (2005) Evaluation of an in situ forming hydrogel wound dressing based on oxidized alginate and gelatin. Biomaterials 26:6335–6342
9. Li Y, Zhu C, Fan D, Fu R, Ma P, Duan Z, Li X, Lei H, Chi L (2020) Construction of porous sponge-like PVA-CMC-PEG hydrogels with pH-sensitivity via phase separation for wound dressing. Int J Polym Mater Polym Biomater 69:505–515
10. Khalilipour A, Paydayesh A (2019) Characterization of polyvinyl alcohol/ZnO nanocomposite hydrogels for wound dressings. J Macromol Sci B 58:371–384
11. Leawhiran N, Pavasant P, Soontornvipart K, Supaphol P (2014) Gamma irradiation synthesis and characterization of AgNP/gelatin/PVA hydrogels for antibacterial wound dressings. J Appl Polym Sci 5:131
12. Sirousazar M, Khadivi H, Delir S (2020) Swelling and drying mechanisms of freeze-thawed polyvinyl alcohol/egg white/montmorillonite bionanocomposite hydrogels. J Macromol Sci B 59:309–330
13. Li W, Wu L, Xu Z, Liu Z (2020) Adhesion-to-fibers and film properties of etherified-oxidized cassava starch/polyvinyl alcohol blends. Iran Polym J 29:331–339
14. Sellappan LK, Anandhavelu S, Doble M, Perumal G, Jeon JH, Vikraman D, Kim HS (2020) Biopolymer film fabrication for skin mimetic tissue regenerative wound dressing applications. Int J Polym Mater Polym Biomater 17:12–18
15. Liu Y, Lv Y, An M, Li F, Lu Y, Song J (2019) Characterization of chitosan-gelatin blend scaffolds. J Macromol Sci B 58:634–644
16. Chen W, Bu Y, Li D, Liu C, Chen G, Wan X, Li N (2019) High-strength, tough, and self-healing hydrogel based on carboxymethyl cellulose. Cellulose 27:853–865
17. Montaser A, Rehan M, El-Naggar ME (2019) pH-Thermosensitive hydrogel based on polyvinyl alcohol/sodium alginate/*N*-isopropyl acrylamide composite for treating re-infected wounds. Int JBbiol Macromol 124:1016–1024
18. Raafat AI, Ali AE-H (2019) A novel Lawsonia inermis (Henna)/(hydroxyethylcellulose/polyvinylpyrrolidone) wound dressing hydrogel: radiation synthesis, characterization and biological evaluation. Polym Bull 76:4069–4086

19. Zeinali A, Sirousazar M, Dastgerdi ZH, Kheiri F (2020) Gelatin/montmorillonite and gelatin/polyvinyl alcohol/montmorillonite bionanocomposite hydrogels: microstructural, swelling and drying properties. J Macromol Sci B 59:263–283
20. Kim I, Yoo M, Seo J, Park S, Na H, Lee H, Kim S, Cho C (2007) Evaluation of semi-interpenetrating polymer networks composed of chitosan and poloxamer for wound dressing application. Int J Pharm 341:35–43
21. Massoumi H, Nourmohammadi J, Marvi MS, Moztarzadeh F (2019) Comparative study of the properties of sericin-gelatin nanofibrous wound dressing containing halloysite nanotubes loaded with zinc and copper ions. Int J Polym Mater Polym Biomater 68:1142–1153
22. Bafandeh MR, Mojarrabian HM, Doostmohammadi A (2019) Poly (vinyl alcohol)/chitosan/akermanite nanofibrous scaffolds prepared by electrospinning. J Macromol Sci B 58:749–759
23. Sirelkhatim A, Mahmud S, Seeni A, Kaus NHM, Ann LC, Bakhori SKM, Hasan H, Mohamad D (2015) Review on zinc oxide nanoparticles: antibacterial activity and toxicity mechanism. Nano-Micro Lett 7:219–242
24. Shitole AA, Raut PW, Khandwekar A, Sharma N, Baruah M (2019) Design and engineering of polyvinyl alcohol based biomimetic hydrogels for wound healing and repair. J Polym Res 26:201
25. Parsa P, Paydayesh A, Davachi SM (2019) Investigating the effect of tetracycline addition on nanocomposite hydrogels based on polyvinyl alcohol and chitosan nanoparticles for specific medical applications. Int J Biol Macromol 121:1061–1069
26. Gao S, Jiang G, Li B, Han P (2018) Effects of high-concentration salt solutions and pH on swelling behavior of physically and chemically cross-linked hybrid hydrophobic association hydrogels with good mechanical strength. Soft Mater 16:249–264
27. Pan H, Fan D, Zhu C, Duan Z, Fu R, Li X (2019) Preparation of physically crosslinked PVA/HLC/SA hydrogel and exploration of its effects on full-thickness skin defects. Int J Polym Mater Polym Biomater 68:1048–1057
28. Schneider LA, Korber A, Grabbe S, Dissemond J (2007) Influence of pH on wound-healing: a new perspective for wound-therapy? Arch Dermatol Res 298:413–420
29. Ono S, Imai R, Ida Y, Shibata D, Komiya T, Matsumura H (2015) Increased wound pH as an indicator of local wound infection in second degree burns. Burns 41:820–824
30. Gethin G (2007) The significance of surface pH in chronic wounds. Wounds UK 3:52
31. Safari J, Zarnegar Z (2014) Advanced drug delivery systems: nanotechnology of health design A review. J Saudi Chem Soc 18:85–99
32. Godoy-Alvarez FK, González-Torres M, Giraldo-Gomez DM, Sánchez-Sánchez R, Pérez-Díaz MA, González-Del Carmen M, Figueroa-González G, Reyes-Hernández OD, Sharifi-Rad J, Cortés H (2021) Synthesis by gamma irradiation of hyaluronic acid-polyvinyl alcohol hydrogel for biomedical applications. Cell Mole Bio 67 (1):58–63
33. Khorasani MT, Joorabloo A, Adeli H, Mansoori-Moghadam Z, Moghaddam A (2019) Design and optimization of process parameters of polyvinyl (alcohol)/chitosan/nano zinc oxide hydrogels as wound healing materials. Carbohydr Polym 207:542–554
34. Glass S, Kühnert M, Abel B, Schulze A (2019) Controlled electron-beam synthesis of transparent hydrogels for drug delivery applications. Polymers 11:501
35. Loh EYX, Mohamad N, Fauzi MB, Ng MH, Ng SF, Amin MCIM (2018) Development of a bacterial cellulose-based hydrogel cell carrier containing keratinocytes and fibroblasts for full-thickness wound healing. Sci Rep 8:2875
36. Hsieh HT, Chang HM, Lin WJ, Hsu YT, Mai FD (2017) Polymethyl methacrylate/polyvinyl alcohol copolymer agents applied on diabetic wound dressing. Sci Rep 7:9531
37. Salimi-Kenari H, Mollaie F, Dashtimoghadam E, Imani M, Nyström B (2018) Effects of chain length of the cross-linking agent on rheological and swelling characteristics of dextran hydrogels. Carbohydr Polym 181:141–149
38. Mahinroosta M, Farsangi ZJ, Allahverdi A, Shakoori Z (2018) Hydrogels as intelligent materials: a brief review of synthesis, properties and applications. Mater Today Chem 8:42–55
39. Eke G, Mangir N, Hasirci N, MacNeil S, Hasirci V (2017) Development of a UV crosslinked biodegradable hydrogel containing adipose derived stem cells to promote vascularization for skin wounds and tissue engineering. Biomaterials 129:188–198
40. Oliveira R, Rouzé R, Quilty B, Alves G, Soares G, Thiré R, McGuinness G (2014) Mechanical properties and in vitro characterization of polyvinyl alcohol-nano-silver hydrogel wound dressings. Interface Focus 4:20130049
41. Rahmati M, Milan PB, Samadikuchaksaraei A, Goodarzi V, Saeb MR, Kargozar S, Kaplan DL, Mozafari M (2017) Ionically crosslinked thermoresponsive chitosan hydrogels formed in situ: a conceptual basis for deeper understanding. Macromol Mater Eng 302:1700227
42. Swaroop K, Somashekarappa H (2018) In vitro biocompatibility and antibacterial activity of gamma ray crosslinked ZnO/PVA hydrogel nanocomposites. Mater Today Proc 5:21314–21321
43. Abdeen ZI, El Farargy AF, Negm NA (2018) Nanocomposite framework of chitosan/polyvinyl alcohol/ZnO: preparation, characterization, swelling and antimicrobial evaluation. J Mol Liq 250:335–343
44. El-Mohdy HA (2013) Radiation synthesis of nanosilver/poly vinyl alcohol/cellulose acetate/gelatin hydrogels for wound dressing. J Polym Res 20:177
45. Zhang L, Wang Z, Xu C, Li Y, Gao J, Wang W, Liu Y (2011) High strength graphene oxide/polyvinyl alcohol composite hydrogels. J Mater Chem 21:10399–10406
46. Mallakpour S, Darvishzadeh M (2018) Nanocomposite materials based on poly (vinyl chloride) and bovine serum albumin modified ZnO through ultrasonic irradiation as a green technique: optical, thermal, mechanical and morphological properties. Ultrason Sonochem 41:85–99
47. Zaid M, Hafiz M, Matori KA, Abdul Aziz SH, Zakaria A, Ghazali M, Sabri M (2012) Effect of ZnO on the physical properties and optical band gap of soda lime silicate glass. Int J Mol Sci 13:7550–7558
48. Singh P, Kumar A, Kaushal A, Kaur D, Pandey A, Goyal R (2008) In situ high temperature XRD studies of ZnO nanopowder prepared via cost effective ultrasonic mist chemical vapour deposition. Bull Mater Sci 31:573–577
49. Kanade K, Kale B, Aiyer R, Das B (2006) Effect of solvents on the synthesis of nano-size zinc oxide and its properties. Mater Res Bull 41:590–600
50. Khozemy EE, Nasef SM, Mahmoud GA (2018) Synthesis and characterization of antimicrobial nanocomposite hydrogel based on wheat flour and poly (vinyl alcohol) using γ-irradiation. Adv Polym Technol 37:3252–3261
51. Razzak MT, Darwis D (2001) Irradiation of polyvinyl alcohol and polyvinyl pyrrolidone blended hydrogel for wound dressing. Radiat Phys Chem 62:107–113